Catal Lett (2008) 122:167–175
DOI 10.1007/s10562-007-9363-7

Gas-phase Hydrodechlorination of Chlorobenzene Over Silica-supported Ni_2P Catalysts Prepared Under Different Reduction Conditions

Jixiang Chen · Shaojun Zhou · Xuguang Liu · Jiyan Zhang

Received: 27 September 2007 / Accepted: 26 November 2007 / Published online: 11 December 2007

Abstract The influence of reduction conditions on the properties and reactivity of silica-supported nickel phosphide (Ni_2P/SiO_2) catalysts for gas-phase hydrodechlorination (HDC) of chlorobenzene was investigated. The catalysts prepared under different reduction conditions had the similar specific surface area ($\sim$370 $m^2\ g^{-1}$), and pore diameter ($\sim$5.2 nm) and Ni_2P crystallites size (10–13 nm). However, comparing with Ni_2P/SiO_2 catalyst prepared at 923 K with the H_2 space velocity of 15,000 mL $g^{-1}\ h^{-1}$ for 2 h, with increasing the H_2 space velocity from 15,000 to 19,200 mL $g^{-1}\ h^{-1}$, or the reduction temperature from 923 to 1023 K or the reduction time from 2 to 6 h, the Ni/P ratio in the prepared catalyst was increased from 1/0.56 to about 1/0.50, and the HDC reaction induction period over the catalyst was also shortened from above 30 to 2–4 h. It is suggested that the induction period might be due to the blocking of active sites by excess phosphorus, which results in hindering the activation of chlorobenzene and the adsorption of hydrogen species on Ni_2P. Under the conditions of 573 K and $W_{Ni}/F_{Cl} = 186.6\ g_{Ni}\ mol_{Cl}^{-1}$ min, the chlorobenzene conversion over the Ni_2P/SiO_2 catalyst reached 99%, and it did not change during 36 h. The good activity and stability of the Ni_2P/SiO_2 catalyst was ascribed to the weak interaction between chlorine and Ni_2P and a great of spilt-over hydrogen species on the catalyst surface.

J. Chen (✉) · S. Zhou · X. Liu · J. Zhang
Department of Catalysis Science and Engineering, School of Chemical Engineering and Technology, Tianjin University, Tianjin 300072, China
e-mail: jxchen@tju.edu.cn

Keywords Nickel phosphide · Chlorobenzene · Hydrodechlorination · Induction period · Reduction conditions

1 Introduction

Chlorinated aromatics are important chemicals that are widely used as solvents and for the synthesis of many organic chemicals, such as odorizers, insect repellents, and fungicides. Their risks to health and the environment have attracted attention due to their acute toxicity and strong bioaccumulation potential; they persist in the environment, accumulate in fatty tissues, and show carcinogenic and mutagenic activity [1]. Therefore, these compounds must be disposed of properly.

In recent years, interest in catalytic hydrodechlorination (HDC) has increased for environmental reasons. Compared with end-of-pipe treatments such as phase transfer or physical separation (adsorption, air or steam stripping, and condensation) and chemical degradation or destruction (thermal incineration and catalytic or wet air oxidation), catalytic HDC has many advantages. These include mild reaction conditions, the transformation of chlorinated compound pollutants to valuable raw materials, and no emission of CO_2 and NO_x [2].

Gas or liquid phase HDC has been used for the disposal of many types of toxic waste, including chlorofluorocarbons, chlorobenzenes, chlorophenols, polychlorinated biphenyls, insecticides, and dioxin/furans. The catalysts used for HDC have mainly been monometallic (e.g. Pt [3–5], Pd [3, 6–9], Rh [10, 11], Ni [12–18]) or bimetallic (e.g. Ni–Au [19], Pd–Ni [20], Pd–Au [21], Pd–Rh [22], Pd–Yb [23], Pd–Fe [24, 25]); supported molybdenum carbide [26] and sulphided Ni–Mo/Al_2O_3 [27] have also been

used. Noble metal catalysts, especially Pd, exhibit HDC activity superior to that of supported nickel-based catalysts; moreover, HDC performance has been shown to be sensitive to Pd dispersion and the nature of the support [28–30]. Keane et al. [31, 32] also found that the hydrodechlorination of chlorobenzene or chlorophenol over supported Ni is structure sensitive. The larger Pd or Ni crystallites are beneficial to the hydrodechlorination rate. In addition, there is an evidence that spilt-over hydrogen species are contributed to the HDC [3, 4, 8, 18, 33–35]. However, whether noble metal or nickel catalysts, an important problem in the application of HDC is catalyst deactivation, which is mainly due to surface poisoning by HCl or/and metal sintering or/and carbon deposition/occlusion of the active sites [11, 17, 36–40]. Thus, the development of solid HDC catalysts that exhibit high and stable activities represents a challenging problem in heterogeneous catalysis.

Transition metal phosphides are novel catalytic materials with excellent performance in hydrodenitrogenation (HDN) and hydrodesulfuration (HDS) [41–48]. Recently, SiO_2-supported Ni_3P and Ni_2P catalysts were used in the HDC of chlorobenzene and showed a good performance [49, 50], the chlorobenzene conversion exceeded 99% under the adopted conditions. Meanwhile, it was found that an induction period occurred for SiO_2-supported Ni_2P catalyst that was prepared from the precursor with Ni/P ratio of 1.0. However, there was no induction period for SiO_2-supported Ni_3P catalyst prepared from the precursor with Ni/P ratio of 3. This indicates that the induction period was perhaps related to the excess P in the Ni_2P catalysts. Because the reduction conditions (H_2 space velocity, reduction temperature and reduction time) can affect the P contents in the prepared catalysts, their influence on the properties of SiO_2-supported Ni_2P was investigated in the present work, and the reasons for the induction period and the good activity of Ni_2P/SiO_2 were also discussed.

2 Experimental

2.1 Catalyst Preparation

The temperature-programmed reduction of nickel phosphate is the usual method for the preparation of nickel phosphide [51]. In the present work, the catalyst precursor with a Ni/P ratio of 1 supported on silica and the supported nickel phosphide were prepared. Firstly, 17.6 g $Ni(NO_3)_2{\cdot}6H_2O$ (60.0 mmol) and 6.92 g $NH_4H_2PO_4$ (60.0 mmol) were dissolved in water, and the precipitate formed was dissolved by a few drops of nitric acid, to obtain 32 mL of aqueous solution; 20.0 g SiO_2 (Qingdao Haiyang Chemical Co. Ltd., China; textural properties shown in Table 2) was then incipiently impregnated with the above aqueous solution and left at room temperature for 12 h. The sample was then dried in air at 393 K for 12 h and calcined in air at 773 K for 4 h, to obtain a supported nickel phosphate precursor. In the next fstep, the nickel phosphate precursor was reduced in a fixed-bed quartz reactor placed in a furnace controlled by a temperature programmer according to the following conditions: the precursor was heated from room temperature to 473 K at 8 K/min and then from 473 K to a final temperature at 1 K/min, and then maintained at this temperature for a certain time. During the reduction, a H_2 (99.999%) flow was set at a rate per gram of precursor. The catalysts prepared under different reduction conditions (including final reduction temperature, reduction time, and H_2 space velocity) are described in Table 1. The mass content of nickel in the catalysts was set at 15% based upon silica. The practical nickel content in the Ni_2P/SiO_2 was measured by an inductively coupled plasma atomic emission spectrometer, and it was about 11%.

As reference, an SiO_2-supported nickel catalyst with a nickel content of 15 wt% (denoted Ni/SiO_2) was also prepared by a procedure similar to that for the supported nickel phosphides except for the final reduction temperature of 723 K.

Before characterization, the fresh catalyst was passivated in a 0.5% O_2/N_2 flow for 6.0 h at room temperature.

2.2 Catalyst Characterization

The reducibility of the catalyst precursor was characterized by hydrogen temperature-programmed reduction (H_2-TPR) in a quartz U-tube reactor, into which a 50 mg sample was loaded. The reduction was conducted in a 10% H_2/N_2 flow of 40 mL/min at a heating rate of 4 K/min, and hydrogen consumption was determined using a thermal conductivity detector (TCD).

Table 1 Ni_2P/SiO_2 catalysts prepared under different reduction conditions

Catalyst	Reduction temperature (K)	Reduction time (h)	H_2 space velocity[a] (mL g^{-1} h^{-1})
Ni_2P-923(2)250	923	2	15,000 (250[b])
Ni_2P-923(4)250	923	4	15,000 (250[b])
Ni_2P-923(6)250	923	6	15,000 (250[b])
Ni_2P-923(2)150	923	2	9,000 (150[b])
Ni_2P-923(2)320	923	2	19,200 (320[b])
Ni_2P-973(2)250	973	2	15,000 (250[b])
Ni_2P-1023(2)250	1,023	2	15,000 (250[b])

[a] Based on the mass of the precursor

[b] H_2 flow rate: mL/min per gram precursor

X-ray diffraction (XRD) patterns of the catalysts were obtained on a Rigaku D/max 2500 V/PC powder diffractometer using Cu-Kα radiation (40 kV, 200 mA). The average size of Ni_2P crystallites was calculated using Scherrer's equation, $d = (0.9\lambda)/(\beta \cos \theta)$, where d is the crystallite size, λ is the wavelength of the radiation, β is the full width at half maximum of the peak, and θ is the Bragg angle.

N_2 adsorption–desorption isotherms of the samples at 77 K were obtained in a Micromeritics TriStar 3, apparatus. Samples were previously degassed for 2 h at 473 K. The Brunauer-Emmett-Teller (BET) equation was used to calculate the specific surface area, S_{BET}. The Barrett-Joyner-Halenda (BJH) method applied over the desorption isotherm was used to determine the mean pore diameter and the pore volume distribution. BET surface area was reproducible to within ±5%.

X-ray photoelectron spectroscopy (XPS) was performed using a PHI-1600 ESCA instrument with Mg-Kα radiation (1253.6 eV). Binding energies were determined with the C1s (284.6 eV) as reference.

Hydrogen temperature-programmed desorption (H_2-TPD) was determined using a commercial TP-D/R/O 1100 SERIES (Finnigan) unit; 400 mg passivated sample was loaded in a quartz reactor and reduced in an H_2 flow at 723 K for 1 h. The sample was then cooled to 303 K and left for 0.5 h in an H_2 atmosphere. H_2-TPD was performed in a 50 mL/min N_2 flow at a heating rate of 10 K/min. The stream from the reactor was dried and the desorbed H_2 was detected with a TCD.

Elemental analysis of the samples was conducted using an inductively coupled plasma atomic emission spectrometer (ICP-9(N + M), Thermo Jarrell-Ash Corp.). The analytic reproducibility was better than ±5%.

2.3 Catalyst Activity Evaluation

The catalytic HDC reaction was performed in an atmospheric fixed-bed quartz reactor (i.d. = 12 mm); 1.0 g catalyst precursor (0.15–0.25 mm in diameter) was supported on quartz cotton and a layer of ceramic beads was placed on the catalyst bed, and it was then reduced in situ as described in Sect. 2.1. Following this preparation procedure, the fresh silica-supported nickel phosphide (0.82) bed was adjusted to the reaction temperature and the feed stream was switched to a mixture of 3 mL/h chlorobenzene and 4.2×10^3 mL/h H_2 (H_2/chlorobenzene molar ratio = 6.5). All the HDC reactions were carried out at an inlet hourly Cl/Ni ratio = 18.8, $W_{Ni}/F_{Cl} = 186.6\ g_{Ni}\ mol_{Cl}^{-1}$ min, where W_{Ni} is the mass of Ni in the catalyst bed and F_{Cl} is the inlet Cl molar flow rate. The experimental results show that the reaction was conducted in the absence of heat/mass transfer limitations. The reactor effluent was absorbed with anhydrous ethanol and analyzed subsequently by a gas chromatograph equipped with a hydrogen flame ionization detector and an OV-101 capillary column, and the analytic reproducibility was better than ±1%.

3 Results and Discussion

3.1 Catalyst Characterization

3.1.1 H_2-TPR Result

In order to prepare Ni_2P phase, surplus phosphorus is necessary due to its loss from the catalysts during TPR process [44, 51]. Thus, in the present investigation, the Ni/P ratio in the catalyst precursor was set at 1. Figure 1 displays the H_2-TPR profile of the Ni_2P/SiO_2 precursor. As a reference, the H_2-TPR trace of the Ni/SiO_2 precursor is shown. There were two reduction peaks centered at 1,050 K and 1,116 K for the Ni_2P/SiO_2 precursor, and there was no peak due to bulk NiO that was usually reduced at about 673 K. In the Ni_2P/SiO_2 precursor, the nickel species might exist in the form of Ni–O–P, and the phosphorus species existed in PO_4^{3-}, and $P_2O_7^{4-}$ and $(PO_3^-)_n$ [52]. These phosphorus species could be reduced to elemental P_4 (P_2) or phosphines P_xH_y, which reacted with nickel species to form nickel phosphide.

3.1.2 XRD Results

Figure 2 shows the XRD patterns of the catalysts. The patterns all showed a broad feature at $2\theta \sim 22°$ due to the amorphous silica. At higher angles, only peaks due to Ni_2P were visible at all catalysts, that is, Ni_2P was formed from

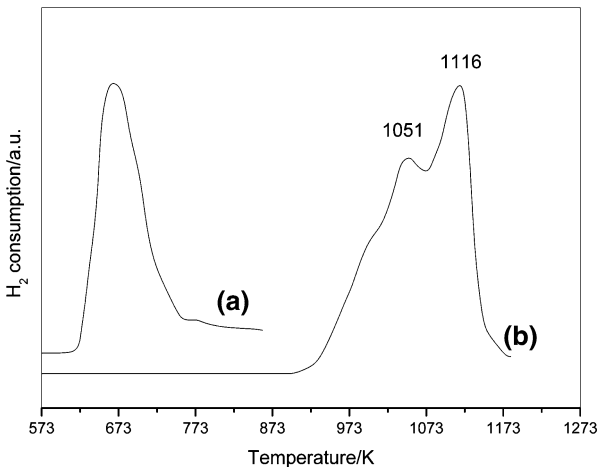

Fig. 1 H_2-TPR profile of catalyst precursor

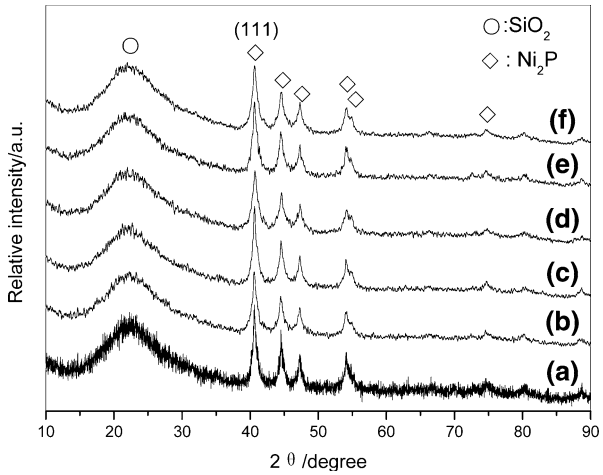

Fig. 2 XRD patterns of Ni_2P/SiO_2 catalysts (a) fresh Ni_2P-923(2)150; (b) fresh Ni_2P-923(2)250; (c) fresh Ni_2P-923(2)320; (d) fresh Ni_2P-923(6)250; (e) fresh Ni_2P-1023(2)250; (f) spent Ni_2P-923(6)250

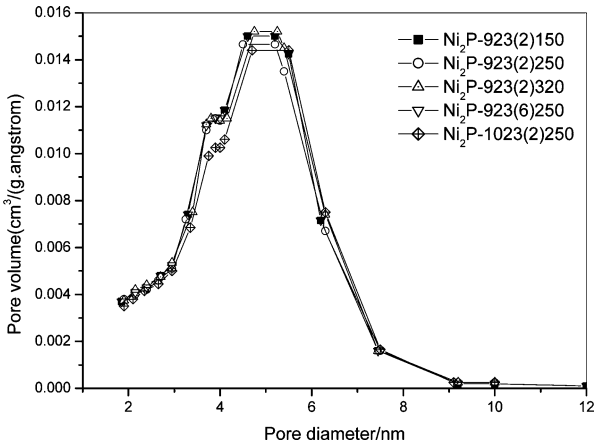

Fig. 3 Pore diameter distribution of catalysts

the precursor at different conditions. This indicates that metal nickel was converted to Ni_2P owing to its reaction with phosphorus species even if it might be formed at low temperature. Based on the reflection of Ni_2P (111), the average sizes of Ni_2P crystallites (shown in Table 2) were calculated using Scherrer equation, and there was no significant difference in Ni_2P crystallite sizes for different catalysts. The XRD results indicate that the reduction conditions did not markedly affect the phases for silica-supported Ni_2P catalysts.

3.1.3 Textural Properties

Table 2 and Fig. 3 show the textural properties and the pore diameter distribution of the catalysts, respectively. Apart from slightly less S_{BET} for Ni_2P-1023(2)250 due to sintering at higher reduction temperature, there was no significant difference in the textural properties, including specific surface area, average pore diameter, average pore volume, and pore diameter distribution. This indicates that the reduction conditions did not make marked influence on the textural properties of Ni_2P/SiO_2 catalysts.

Table 2 also shows the Ni/P molar ratios in the catalysts. With increasing H_2 space velocity, reduction temperature, and reduction time, Ni/P ratios in the catalysts were increased, indicating that a P loss occurred. The effect of H_2 space velocity was related to the mass transfer. During the reduction, H_2O formed from the oxidic Ni and phosphate species and the pores of the support hindered the diffusion of the H_2O. The higher the vapor pressure of H_2O within the pores is, the more the equilibria are shifted to the side of the oxidic Ni and phosphate species [52]. Thus, an increasing in the H_2 space velocity facilitates the quicker removal of the water as well as P_xH_y (or P_2) formed upon reduction, which was in favor of increasing Ni/P ratios.

Table 2 Textural properties and Ni/P molar ratio of Ni_2P/SiO_2 catalysts prepared under different reduction conditions

Sample	Ni_2P Particle size[a] (nm)	S_{BET} ($m^2\ g^{-1}$)	Pore diameter (nm)	Pore volume ($cm^3\ g^{-1}$)	Ni/P Molar ratio[b]	Ni/P Molar ratio in bulk[d]
SiO_2	–	548	5.5	0.797	–	–
Ni_2P-923(2) 150	13.2	368	5.4	0.499	1.0	–[e]
Ni_2P-923(2) 250	11.8	370	5.2	0.479	1.3	1/0.56
Ni_2P-923(2) 320	10.7	379	5.2	0.495	–	1/0.50
Ni_2P-923(6) 250	12.8	370	5.2	0.483	1.3	1/0.48
Ni_2P-1023(2) 250	11.7	352	5.4	0.479	–[c]	1/0.49

[a] Calculated with Scherrer formula using (111) reflection of Ni_2P

[b] Ni/P atomic ratio on catalyst surface

[c] No phosphorus was detected

[d] Ni/P atomic ratio in the catalyst measured by ICP

[e] No measure

3.1.4 XPS Results

XPS results indicate that there were two electronic binding energies of $Ni2p_{3/2}$ on the surface of the catalysts, i.e., 856.5 and 853.0 eV, and there were also two electronic binding energies of $P2p_{3/2}$. These results were similar to those reported by Bussell et al. [44, 53] and Smith et al. [54]. All catalysts possessed oxidized Ni and P species because after synthesis, they were passivated using 0.5% O_2 in N_2 to protect them from deep oxidation. The value at 856.5 eV was assigned to Ni^{2+} in the oxide layer formed on the nickel phosphide particles during passivation period. The other one at 853.0 eV was higher than that of $Ni2p_{3/2}$ in nickel metal (852.5–852.9 eV) but lower than that of $Ni2p_{3/2}$ in NiO (853.5–854.1 eV) [44], which indicated that the Ni species had a partial positive charge ($Ni^{\delta+}$). For two electronic binding energies of $P2p_{3/2}$, one was about 134.4 eV, and the other was about 129.5 eV. The former was due to P^{5+} species, and the latter was less than the value for elemental phosphorus (130.2 eV); that is, the P had a small negative charge ($P^{\delta-}$). The above results show that there was a transfer of electron density from Ni to P in Ni_2P, which is of characteristic for nickel phosphides [55–57]. The DFT studies [48] indicate that the Ni–P bonds in Ni_2P are covalent; that is, there is a "ligand effect" for Ni–P bonds. However, this effect is weak, and Ni_2P behaves as a metal.

Although the Ni_2P phase existed in all catalysts, the Ni/P ratio (shown in Table 2) on the surface of the catalysts prepared under different conditions had a large difference. With increasing H_2 space velocity, the Ni/P ratio on the catalyst surface gradually increased, and no significant phosphorus was detected on the surface of Ni_2P-923(2)320. This indicates that an increased H_2 space velocity favored the loss of phosphorus from the catalyst surface, which was related to the mass transfer as above-mentioned in Sect. 3.1.3. Also, phosphorus was not detected on the surface of Ni_2P-1023(2)250, indicating that higher reduction temperature also led to the loss of P from the catalyst surface. However, there was no evident influence of reduction time on the Ni/P ratio on the catalyst surface.

3.1.5 H2-TPD Results

The H_2-TPD profiles of different catalysts are shown in Fig. 4. H_2-TPD is an effective approach to unraveling the heterogeneity of a catalyst surface and the nature of the interaction between hydrogen species and such surfaces. All of the H_2-TPD profiles include two desorption peaks, one below 673 K and one above 673 K. Generally, the hydrogen species desorbed below 600 K were ascribed to those on the metal surface, while those desorbed above 600 K were ascribed to spilt-over hydrogen species. Hydrogen spillover is now well established for supported transition metal catalysts where H_2 dissociates on the metal into atomic hydrogen, which then spills over onto the (typically) oxide support [58–60]. During the H_2-TPD process, the spilt-over hydrogen species can diffuse from the support surface to the metal surface, which was termed as 'reverse spillover' [59], and were then recombined and desorbed from the metal surface.

There was a difference in H_2-TPD results between different catalysts. Ni_2P behaves as a metal and can adsorb hydrogen dissociatedly. Comparing with Ni_2P-923(2)250, H_2 desorption amount at low temperature were greater over Ni_2P-923(2)320, Ni_2P-923(6)250, andNi_2P-1023(2)250; that is, there were relatively less hydrogen species adsorbed on Ni_2P phase in Ni_2P-923(2)250. However, Ni_2P923(2)-250 had more spilt-over hydrogen species than other catalysts. This finding indicates that the reduction conditions had a marked effect on the surface properties of Ni_2P/SiO_2 catalysts. Considering the Ni/P molar ratio both on the surface and in the bulk of the catalysts as shown in Table 2, it is suggested that excess P perhaps covered Ni_2P crystallites surface, and the higher reduction temperature, longer reduction time and larger H_2 space velocity promoted P loss. Therefore, hydrogen species adsorbed on Ni_2P was more in Ni_2P-923(2)320, Ni_2P-923(6)250, and Ni_2P-1023(2)250.

Compared with Ni/SiO_2 catalyst [49], Ni_2P/SiO_2 catalysts had more spilt-over hydrogen species. Spillover is a common phenomenon with supported catalysts. According to the mechanism of hydrogen spillover [61], on the surface of Ni_2P/SiO_2, hydrogen species spilled over across the interface between the Ni_2P crystallites and the SiO_2

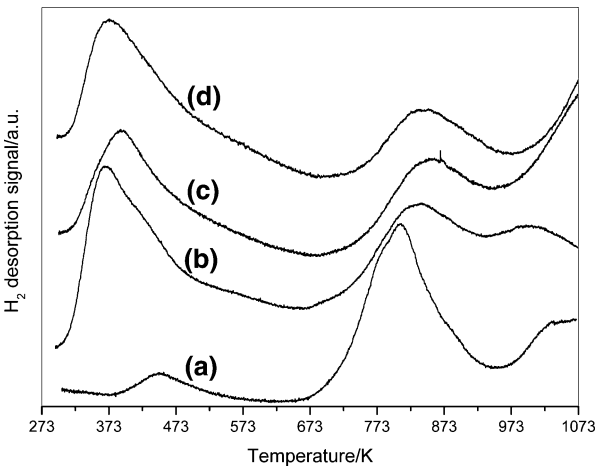

Fig. 4 H_2-TPD profiles of Ni_2P/SiO_2 catalysts (a) Ni_2P-923(2)250; (b) Ni_2P-923(2)320; (c) Ni_2P-923(6)250; (d) Ni_2P-1023(2)250

support. During the spillover, the bonds between the dissociated hydrogen species and the Ni_2P surface were broken, and bonds between the hydrogen species and the silica surface were formed. There is an energy barrier for spillover [61] that depends on the interaction between the hydrogen species and the activating/accepting surfaces and on the diffusion ability of the hydrogen species. In Ni_2P, P withdraws electron from the metal nickel, thereby lowering the Fermi energy level of the nickel [48]; thus, the interaction between the dissociated hydrogen species and Ni_2P would be weaker than that with the metal nickel. This can be confirmed by the initial adsorption heat of H_2 adsorbed on Ni and Ni_2P, which is estimated to be 85 and 64 kJ/mol [62], respectively. DFT calculations [55] also show that H adsorption on Ni_2P was slightly weaker than that on Ni. In addition, the dissociated hydrogen species would diffuse exclusively through the Ni–Ni bridge site when they migrate on the metal Ni surface [63]. Due to the weaker interaction between hydrogen species and the Ni–P bridge site [55], the diffusion of dissociated hydrogen species over the Ni–P bridge site is easier than that over a Ni–Ni bridge site; that is, dissociated hydrogen species migrate more easily on a nickel phosphide surface than on a metal nickel surface. Therefore, it is suggested that the hydrogen species adsorbed on nickel phosphides easily spill over to the support surface, and the support became a reservoir of hydrogen species.

3.1.6 Catalyst Activity

The activities of the Ni_2P/SiO_2 catalysts in the HDC of chlorobenzene are shown in Fig. 5. There was a large difference in the initial chlorobenzene conversion over the catalysts prepared under different conditions, and the initial rates over the Ni_2P-923(6)250, Ni_2P-1023(2)250, Ni_2P-923(4)250, Ni_2P-973(2)250, Ni_2P-923(2)320, and Ni_2P-923(2)250 and Ni_2P-923(2)150 were 8.7×10^{-5}, 7.8×10^{-5}, 6.5×10^{-5}, 6.3×10^{-5}, 4.7×10^{-5}, 3.7×10^{-5} and 1.7×10^{-5} $mol_{Cl}\ g_{Ni}^{-1}\ s^{-1}$. However, the chlorobenzene conversion increased along with the reaction and exceeded 99% except Ni_2P-923(2)150 whose chlorobenzene conversion reached above 95% at 36 h. Ni_2P/SiO_2 possessed excellent activity and stability in the hydrodechlorination, which was superior to other metal catalysts. Our study [49] showed that the chlorobenzene was about 80% over 15 wt% Ni/SiO_2 under the same reaction conditions. Noble metal catalysts, especially Pd, exhibit good gas-phase HDC activity under the more mild temperature (413–473 K), however, their deactivation also occurred, such as Pd/ZrO_2 [9], Pd/CeO_2 [64], Ln–Pd/SiO_2 (Ln = La, Ce, Sm, Eu, Gd and Yb) [65].

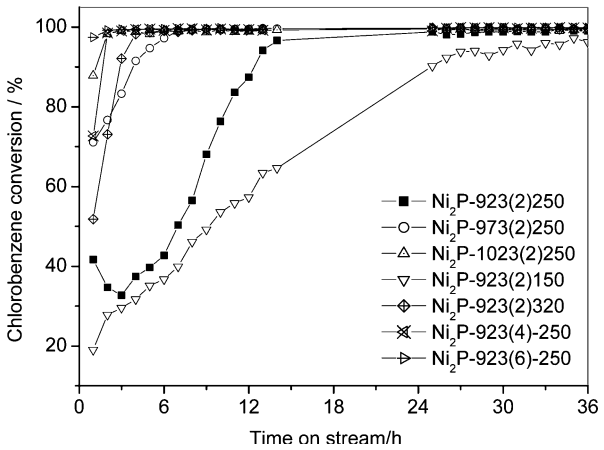

Fig. 5 Catalytic HDC activity of Ni_2P/SiO_2 catalysts. Reaction conditions: 573 K, inlet hourly Cl/Ni ratio = 18.8, W_{Ni}/F_{Cl} = 186.6 $g_{Ni}\ mol_{Cl}^{-1}$ min

Figure 5 also shows that there was an induction period in HDC. Moreover, there is a trend that the initial chlorobenzene conversion was higher and the induction period was shorter over the catalysts prepared with the larger H_2 space velocity, the higher final reduction temperature, and the longer reduction time. Comparing with the Ni/P molar ratio and the hydrogen species on the surface of different catalysts, it can be suggested that the lower initial activity and the longer induction period was related to the higher phosphorus content and less hydrogen species on Ni_2P crystallites in the fresh catalysts. Surplus P could cover the active sites and block the reaction. This covering perhaps occurred on the surface of Ni_2P as above-mentioned, whereas the P loss from Ni_2P surface was favored by increasing reduction temperature, reduction time, and H_2 space velocity during the reduction. This also led to an increasing hydrogen species adsorbed on Ni_2P. During the course of reaction, the active sites would be recovered or the catalysts would be activated. The Ni/P molar ratios in the fresh and used Ni_2P-923(2)250 were measured to be 1/0.56 and 1/0.52, respectively. This means that a phosphorus loss occurred during the HDC reaction. As shown in Fig. 6, H_2 desorption amount below 673 K was much larger over used Ni_2P-923(2)250 than that over fresh Ni_2P-923(2)250. This indicates that more hydrogen species adsorbed on Ni_2P crystallites after reaction, which was perhaps related to P loss. P loss also was found on silica-supported nickel phosphide during HDS [66]. In addition, there was a shift of TPD peak due to spilt-over hydrogen species to higher temperature for the used catalyst (Fig. 6). This perhaps was related to the change in the surface of the catalyst after reaction, which influence the desorption of the spilt-over hydrogen species. The above results indirectly indicate that the chlorobenzene could be activated and attacked by hydrogen species on Ni_2P.

Chlorine is known [67, 68] to act as an electron acceptor with respect to transition metals, and the adsorption strength of chlorine is enhanced as the electronic density of the metal atom increases, however, which is not beneficial to the reduction of the metal chloride. Coq et al. and Bodnariuk et al. [67, 68] proposed a mechanism for the hydrogenolysis of chlorobenzene over supported Pd, Rh, Pd–Rh and Pd–Sn catalysts as following:

$$C_6H_5Cl(g) + Z - H \rightarrow C_6H_6(g) + Z - Cl$$

$$Z - Cl + H_2(g) \rightarrow Z - H + HCl(g)$$

$$Z - H + HCl(g) \rightarrow Z - Cl + H_2(g)$$

where Z represents a surface site, especially a metal site. The strong interaction between Z and Cl inhibits the desorption of Cl, that is, a self-inhibition of the active surface by a strong but reversible interaction between HCl and the metal. A higher electron density of the Pd atom in PdSn catalyst can stabilize the adsorption of chlorine, which results in a lower reducibility of the surface. As a result, the activation energy of PdSn catalyst in hydrodechlorination is higher than that of Pd catalyst. Due to nickel bearing a small positive charge in Ni_2P, the interaction between chlorine and nickel can be weaker than that in metal nickel, which would favor the poison resistance of nickel phosphide to chlorine; in other words, chlorine desorbs easily from a nickel phosphide surface. Besides, the "doping effect" of P was also beneficial in decreasing the coverage of chlorine on nickel sites and so in decreasing the self-inhibition of the active sites owing to Cl. It is generally accepted that metal nickel can be poisoned by chlorine and be transformed into $NiCl_2$ [69, 70], whereas this phenomenon can be inhibited for Ni_2P due to the interaction between P and Ni. As shown in the XRD pattern (Fig. 1f) of the spent Ni_2P-923(6)250, there were only SiO_2 and Ni_2P, and the Ni_2P crystallites size was similar to that in the fresh Ni_2P-923(6)250. These indicate that silica-supported Ni_2P possessed good structural stability during the HDC of chlorobenzene.

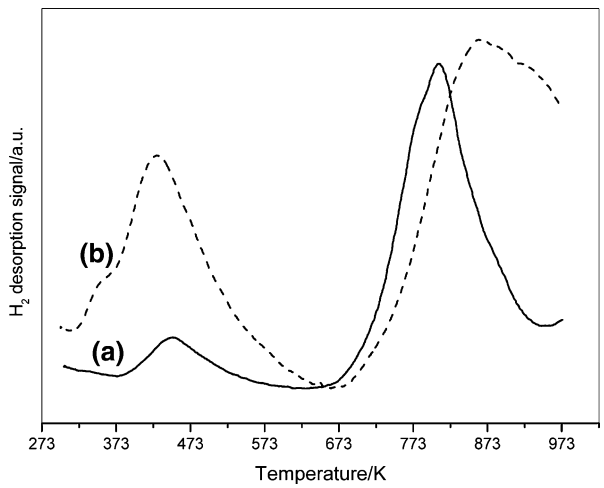

Fig. 6 H_2-TPD profiles of (a) fresh Ni_2P-923(2)250 and (b) spent Ni_2P-923(2)250

As shown in H_2-TPD, compared with Ni/SiO_2, Ni_2P/SiO_2 catalyst has more spilt-over hydrogen species. There has been evidence in the literature of the contribution of spilt-over hydrogen species to HDC [3, 4, 8, 18, 33–35] although the chemical nature of the spilt-over hydrogen species is a subject of controversy [71]. For example, Keane et al. [34] showed that spilt-over hydrogen species contributed to gas phase hydrodechlorination over $Ni/SiO_2 + SiO_2$ physical mixtures. The reaction rates (per unit mass Ni) are enhanced by extending the Ni/SiO_2–SiO_2 interface, and a non-contiguous combination does not deliver any beneficial effect. Shin et al. and Keane et al. [58, 34] also considered that spilt-over hydrogen species appeared to be hydrogenolytic in nature and were responsible for promoting HDC, and they proposed a reaction scheme involving spilt-over hydrogen species as following:

$$C_6H_5Cl(g) + S \rightarrow C_6H_5Cl - S$$

$$H_2(g) + S' \rightleftharpoons 2H - S'$$

$$C_6H_5Cl - S + 2H - S' \rightarrow C_6H_6(g) + HCl - S + 2S'$$

$$C_6H_5Cl(g) + HCl - S \rightleftharpoons HCl(g) + C_6H_5Cl - S$$

where S represents a surface site adsorbing chlorobenzene, S' represents a surface site associating with spilt-over hydrogen species. The surface reaction occurred between non-competitively and dissociatively adsorbed chlorobenzene and spilt-over hydrogen species. A kinetic study [33] also showed a similar result. As to Ni_2P/SiO_2 catalysts, whether chlorobenzene adsorbs on Ni_2P, the support or the interface of Ni_2P and the support, abundant spilt-over hydrogen species can promote the hydrogenolysis of C–Cl. There was more spilt-over hydrogen species formed on the spent catalyst than those on the fresh catalyst (shown Fig. 6). Shin et al. [58] found a similar phenomenon. This also supports the promoting role of spilt-over hydrogen species on the hydrogenolysis of C–Cl. In addition, chloride ions would be converted to HCl in the reaction with spilt-over hydrogen species [3], that is, spilt-over species had a role for "cleaning" of chlorine ions from the surface of the catalyst.

Summarizing the above results, there is a strong suggestion that the weak interaction between chlorine and Ni_2P and abundant spilt-over hydrogen species promote the hydrodechlorination over Ni_2P/SiO_2.

4 Conclusions

The reduction conditions did not made a marked effect on textural properties of Ni_2P/SiO_2; however, they greatly influenced the surface properties of the catalysts, which resulted in different initial activities and reaction induction periods over the different catalysts. With increasing the H_2 space velocity, and reduction temperature and reduction time during the catalyst preparation, the P/Ni ratio in the catalyst was decreased, and hydrogen species adsorbed on Ni_2P was increased. As a result, the induction period was shortened. The induction period might be due to the blocking of active sites by excess phosphorus, which might hinder the activation of chlorobenzene and the adsorption of hydrogen species on Ni_2P.

Ni_2P/SiO_2 showed not only excellent activity but also good stability in hydrodechlorination, which can be attributed to the weak interaction between chlorine and Ni_2P and a great of spilt-over hydrogen species on the catalyst surface.

References

1. Kawabata T, Atake I, Ohishi Y, Shishido T, Tian Y, Takaki K, Takehira K (2006) Appl Catal B 66:151
2. Keane MA (2004) Appl Catal A Gen 271:109
3. Hashimoto Y, Uemichi Y, Ayame A (2005) Appl Catal A Gen 287:89
4. Hashimoto Y, Ayame A (2003) Appl Catal A Gen 250:247
5. Yoneda T, Takido T, Konuma K (2007) J Mol Catal A Chem 265:80
6. Calvo L, Gilarranz MA, Casas AJ, Mohedano AF, Rodríguez JJ (2006) Appl Catal B Environ 67:68
7. Kawabata T, Atake I, Ohishi Y, Shishido T, Tian Y, Takaki K, Takehira K (2006) Appl Catal B Environ 66:151
8. Amorim C, Yuan G, Patterson PM, Keane MA (2005) J Catal 234:268
9. Gopinath R, Lingaiah N, Babu NS, Suryanarayana I, Sai Prasad SP, Obuchi A (2004) J Mol Catal A Chem 223:289
10. Yuan G, Keane MA (2003) Catal Commun 4:195
11. Coq B, Ferrat G, Figueras F (1986) J Catal 101:434
12. Wu WH, Xu J, Ohnishi R (2005) Appl Catal B Environ 60:129
13. Chary KVR, Rao PVR, Vishwanathan V (2006) Catal Commun 7:974
14. Kim P, Kim YH, Kim H, Song IK, Yi J (2005) J Mol Catal A Chem 231:247
15. Keane MA, Pina G, Tavoularis G (2004) Appl Catal B Environ 48:275
16. Shin EJ, Keane MA (1998) Appl Catal B Environ 18:241
17. Cesteros Y, Salagre P, Medina F, Sueiras JE (2) Appl Catal B Environ 25:213
18. Chary KVR, Lakshmi KS, Rao PVR, Rao KSR, Papadaki M (2004) J Mol Catal A Chem 223:353
19. Yuan G, Louis C, Delannoy L, Keane MA (2007) J Catal 247:256
20. Simagina V, Likholobov V, Bergeret G, Gimenez MT, Renouprez A (2003) Appl Catal B Environ 40:293
21. Nutt MO, Heck KN, Alvarez P, Wong MS (2006) Appl Catal B: Environ 69:115
22. Pozan GS, Boz I (2006) J Hazard Mater 136:917
23. Jujjuri S, Ding E, Hommel EL, Shore SG, Keane MA (2006) J Catal 239:486
24. Golubina VE, Lokteva ES, Lunin VV, Telegina SN, Yu Stakheev A, Tundo P (2006) Appl Catal A Gen 302:32
25. Wei JJ, Xu XH, Liu Y, Wang DH (2006) Water Res 40:348
26. de Lucas Consuegra A, Patterson PM, Keane MA (2006) Appl Catal B Environ 65:227
27. Gryglewicz G, Stolarski M, Gryglewicz S, Klijanienko A, Piechocki W, Hoste S, Van Driessche I, Carleer R, Yperman J (2006) Chemosphere 62:135
28. Halligudi SB, Devassay BM, Ghosh A, Ravikumar V (2002) J Mol Catal A Chem 184:175
29. Gopinath R, Rao KN, Prasad PSS, Madhavendra SS, Narayanan S, Vivekanandan G (2002) J Mol Catal A Chem 181:215
30. Juszczyk W, Malinowski A, Karpiński Z (1998) Appl Catal A Gen 166:311
31. Keane MA, Park C, Menini C (2003) Catal Lett 88:89
32. Pina G, Louis C, Keane MA (2003) Phys Chem Chem Phys 5:1924
33. Keane AM, Yu Murzin D (2001) Chem Eng Sci 56:3185
34. Keane MA, Tavoularis G (2003) React Kinet Catal Lett 78:11
35. Kovenklioglu S, Cao Z, Shah D, Farrauto RJ, Balko EN (1992) AIChE J 38:1003
36. Menini C, Park C, Shin EJ, Tavoularis G, Keane MA (2000) Catal Today 62:355
37. Gampine A, Eyman DP (1998) J Catal 179:315
38. Murthy KV, Patterson PM, Jacobs G, Davis BH, Keane MA (2004) J Catal 223:74
39. Consuegra ADL, Patterson PM, Keane MA (2006) Appl Catal B Environ 62:57
40. Urbano FJ, Marinas JM (2001) J Mol Catal A Chem 173:329
41. Oyama ST (2003) J Catal 216:343
42. Yang SF, Liang CH, Prins R (2006) J Catal 237:118
43. Wang AJ, Ruan LF, Teng Y, Li X, Lu MH, Ren J, Wang Y, Hu YK (2005) J Catal 229:314
44. Sawhill SJ, Layman KA, Van Wyk DR, Engelhard MH, Ch Wang M, Bussell ME (2005) J Catal 231:300
45. Shu YY, Lee Y-K, Oyama ST (2005) J Catal 236:112
46. Lee Y-K, Shu YY, Oyama ST (2007) Appl Catal A Gen 322:191
47. Wang X, Clark P, Oyama ST (2002) J Catal 208:321
48. Liu P, Rodriguez JA, Asakura T (2005) J Phys Chem B 109:4575
49. Liu XG, Chen XJ, Zhang YJ (2007) Catal Commun 8:1905
50. Zhou SJ, Chen JX, Liu XG, Zhang YJ (2007) Chin J Catal 28:498
51. Oyama ST, Wang X, Lee YK, Bando K, Requejo FG (2002) J Catal 210:207
52. Stinner C, Tang Z, Haouas M, Weber T, Prins R (2002) J Catal 208:456
53. Sawhill SJ, Phillips DC, Bussell ME (2003) J Catal 215:208
54. Abu II, Smith KJ (2007) Catal Today 125:248
55. Liu P, Rodriguez AJ (2005) J Am Chem Soc 127:14871
56. Rodriguez JA, Kim JY, Hanson JC, Sawhill SJ, Bussell ME (2003) J Phys Chem B 107:6276
57. Layman KA, Bussell ME (2004) J Phys Chem B 108:10930
58. Shin E, Spiller A, Tavoularis G, Keane MA (1999) Phys Chem Chem Phys 1:3173
59. Arai M, Fukushima M, Nishiyama Y (1996) Appl Surf Sci 99:145
60. Paál Z, Menon GP (1983) Catal Rev Sci Eng 25:229
61. Conner WC, Falconer JL (1995) Chem Rev 95:759
62. Shen J, Spiewak BE, Dumesic JA (1997) Langmuir 13:2735
63. Watson GW, Wells RPK, Willock DJ (2001) J Phys Chem B 105:4889
64. Gopinath R, Lingaiah N, Sreedhar B, Suryanarayana I, Sai Prasad PS, Obuchi A (2003) Appl Catal B Environ 46:587
65. Jujjuri S, Ding E, Shore SG, Keane MA (2007) J Mol Catal A Chem 272:96
66. Oyama TS, Wang X, Lee Y-K, Chun W-J (2004) J Catal 221:263

67. Coq B, Ferrat G, Figueras F (1986) J Catal 101:434
68. Bodnariuk P, Coq B, Ferrat G, Figueras F (1989) J Catal 116:459
69. Cesteros Y, Salagre P, Medina F, Sueiras EJ, Tichit D, Coq B (2001) Appl Catal B 32:25
70. Choi YH, Lee WY (2001) J Mol Catal A 174:193
71. Roland U, Braunschweig T, Roessner F (1997) J Mol Catal A Chem 127:61